A review: The comparison between alkali-activated slag (Si + Ca) and metakaolin (Si + Al) cements

Chao Li [a,*], Henghu Sun [a,b], Longtu Li [a]

[a] State Key Laboratory of New Ceramics and Fine Processing, Department of Materials Science and Engineering, Tsinghua University, Beijing 100084, China
[b] School of Engineering and Computer Science, University of the Pacific, Stockton, CA 95211, USA

ARTICLE INFO

ABSTRACT

There are two main models of alkali-activated cements, one is the case of the activation of slag (Si + Ca) and the other is activation of metakaolin (Si + Al). This paper reviews current knowledge about the comparison between alkali-activated slag (Si + Ca) and metakaolin (Si + Al) cements, including the general properties of slag and metakaolin, hydration products reaction mechanisms, and the role of Ca and Al.

© 2010 Elsevier Ltd. All rights reserved.

Contents

1. Introduction

Alkali-activated cements have a history starting from the 1940's, and Table 1 summarizes a historical background about important events in the development of alkali-activated cements [1]. We classify this new kind of binders as the third generation cement after lime and ordinary Portland cement (OPC), and it is now accepted that alkali-activated cements have emerged as an alternative to OPC, which seems to have superior durability and environmental performance.

Because of these advantages, alkali-activated cements have found a variety of applications, Krivenko [2] summarizes the numerous applications of alkali-activated cements, such as transportation, industrial, agricultural, residential, mining, oil well cements, high-volume applications and so on. Besides, one of the major newer applications is in waste management, including radioactive wastes management and immobilization of toxic metals [3–6].

Theoretically, any material composed of silica and aluminum can be alkali-activated. So far, the investigations performed have used the

* Corresponding author. Room 2609, YIFU Science and Technology Building, Tsinghua University, Beijing 100084, China. Tel./fax: +86 10 62794738.
E-mail address: chao-li07@mails.tsinghua.edu.cn (C. Li).

Table 1
Bibliographic history of some important events about alkali-activated cements.

Author	Year	Significance
Feret	1939	Slags used for cement.
Purdon	1940	Alkali–slag combinations.
Glukhovsky	1959	Theoretical basis and development of alkaline cements.
Glukhovsky	1965	First called "alkaline cements".
Davidovits	1979	"Geopolymer" term.
Malinowski	1979	Ancient aqueducts characterized.
Forss	1983	F-cement (slag–alkali–superplasticizer).
Langton and Roy	1984	Ancient building materials characterized.
Davidovits and Sawyer	1985	Patent of "Pyrament" cement.
Krivenko	1986	DSc thesis, R_2O–RO–SiO_2–H_2O.
Malolepsy and Petri	1986	Activation of synthetic melilite slags.
Malek et al.	1986	Slag cement-low level radioactive wastes forms.
Davidovits	1987	Ancient and modern concretes compared.
Deja and Malolepsy	1989	Resistance to chlorides shown.
Kaushal et al.	1989	Adiabatic cured nuclear wastes forms from alkaline mixtures.
Roy and Langton	1989	Ancient concretes analogs.
Majundar et al.	1989	$C_{12}A_7$–slag activation.
Talling and Brandstetr	1989	Alkali-activated slag.
Wu et al.	1990	Activation of slag cement.
Roy et al.	1991	Rapid setting alkali-activated cements.
Roy and Silsbee	1992	Alkali-activated cements: an overview.
Palomo and Glasser	1992	CBC with metakaolin.
Roy and Malek	1993	Slag cement.
Glukhovsky	1994	Ancient, modern and future concretes.
Krivenko	1994	Alkaline cements.
Wang and Scivener	1995	Slag and alkali-activated microstructure.
Shi	1996	Strength, pore structure and permeability of alkali-activated slag.
Fernández-Jiménez and Puertas	1997	Kinetic studies of alkali-activated slag cements.
Katz	1998	Microstructure of alkali-activated fly ash.
Davidovits	1999	Chemistry of geopolymeric systems, technology.
Roy	1999	Opportunities and challenges of alkali-activated cements.
Palomo	1999	Alkali-activated fly ash — a cement for the future.
Gong and Yang	2000	Alkali-activated red mud–slag cement.
Puertas	2000	Alkali-activated fly ash/slag cement.
Bakharev	2001–2002	Alkali-activated slag concrete.
Palomo and Palacios	2003	Immobilization of hazardous wastes.
Grutzeck	2004	Zeolite formation.
Sun	2006	Sialite technology.
Duxson	2007	Geopolymer technology: the current state of the art.
Hajimohammadi, Provis and Devente	2008	One-part geopolymer.
Provis and Deventer	2009	Geopolymers: structure, processing, properties and industrial applications.

following prime materials: blast furnace slag, metakaolin, fly ash, kaolinitic clays and red mud. Depending on the composition of prime materials, earlier Krivenko, quoted by Roy [1], prefers to separate the binding systems into two groups: Me_2O–MeO–Me_2O_3–SiO_2–H_2O and Me_2O–Me_2O_3–SiO_2–H_2O. While for Palomo et al. [7], they also establish two models of alkali-activated binding systems. The first one is the case of the activation of blast furnace slag $(Si + Ca)$ with mild alkaline solution, having CSH as the main reaction products. In the second model of alkali activation $(Si + Al)$, the general example is the alkali activation of metakaolin or Class F fly ash with medium to high alkaline solutions, and the reaction products are zeolite like polymers. Davidovits named the second group as "Geopolymer" since they have polymeric structure [8].

These two types of cements have attracted a lot of attention from all over the word due to their special characteristics, and known as the typical representation of alkali-activated cements. This paper reviews the comparison between alkali-activated slag $(Si + Ca)$ and metakaolin $(Si + Al)$ cements, including the general properties of slag and metakaolin, hydration products, reaction mechanisms, and the role of Ca and Al.

2. General properties of slag and metakaolin

The first book about alkali-activated cements and concretes by Shi et al. [9] has discussed the detailed general properties of slag and metakaolin. Provis and Deventer [10] also summarized the properties of raw materials used in geopolymer manufacture in their new book: Geopolymers: structure, processing, properties and industrial applications.

2.1. Ground granulated blast furnace slag (GGBFS)

2.1.1. The production of GGBFS

Blast furnace slag is produced from the manufacture of pig iron. It forms when slagging agents (e.g., iron ore, coke ash, and limestone) are added to the iron ore to remove impurities. In the process of reducing iron ore to iron, a molten slag forms as a nonmetallic liquid (consisting primarily of silicates and aluminosilicates of calcium and other bases) that floats on top of the molten iron. The molten slag is then separated from the liquid metal and cooled. Depending on the cooling method, three types of slag are produced, namely aircooled, expanded, and granulated [11]. If the molten slag is quenched sufficiently rapidly by water, the ground product is known as ground granulated blast furnace slag (GGBFS). It is classified as a latent hydraulic material, meaning it has pozzolanic, cementitious properties. GGBFS is ground to improve its reactivity during cement hydration and widely used as a supplementary cementitious material in Portland cement concrete.

2.1.2. Glass phase and reactivity

Slag is generated in the blast furnace and subsequently quenched, and its composition is essentially that of an over-charge-balanced calcium aluminosilicate framework. The chemical component of GGBFS consists mainly of the CaO–SiO_2–MgO–Al_2O_3 system, and is described as a mixture of phases with compositions resembling gehlenite $(2CaO \cdot Al_2O_3 \cdot SiO_2)$ and akermanite $(2CaO \cdot MgO \cdot 2SiO_2)$, as well as a depolymerized calcium aluminosilicate glass.

The key glass network forming cations are Si^{4+} and Al^{3+}, and the divalent Ca^{2+} and Mg^{2+} act as network modifiers along with any alkalis present. Many researches [12,13] have proved that the reactivity of different slags in alkali-activated materials mostly depend on their phase composition and glass structure. But, there is no relationship between reactivity and glass phase content. It has been heuristically reported that the glass content of the slag should be in excess of 90% to show satisfactory properties. While other research data show that slag samples with as little as 30–65% glass contents are still suitable, but no specific minimum required glass content appears to emerge from these tests [14]. Pol et al. [15] concluded that although a glassy structure is essential to reactivity, research has shown that there is no exact correlation of glass content to hydraulicity, and therefore, there is no guarantee that a high glass content will produce a highly reactive slag. However, there is one thing we can confirm that the degree of depolymerization (DP) largely controls reactivity. A formula is described as follow:

$$DP = \frac{n(CaO) - 2n(MgO) - n(Al_2O_3) - n(SO_3)}{n(SiO_2) - 2n(MgO) - 0.5n(Al_2O_3)} \quad (1)$$

This ration is typically in the range of 1.3–1.5 for GGBFS, with higher values indicating a more depolymerized and therefore, more silicate network [16]. While there are a number of ways to describe the degree of depolymerization, and the very common and useful method is parameterized with the mean number of non-bridging oxygen (NBO)/tetrahedron [17] or by the fraction of non-bridging oxygen that is determined simply from the concentrations of network-modifying cations (Ca^{2+}, Na^+, etc.) [18,19]. With the development of NMR test

technology, O-17 NMR analysis provides a convenient way to describe the polymerization of aluminosilicate glasses [20,21].
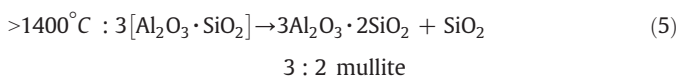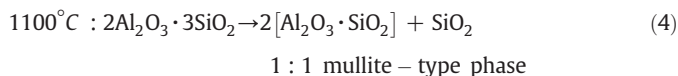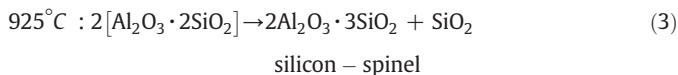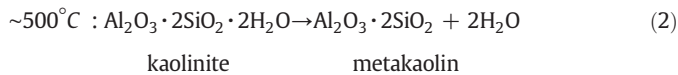
Moreover, the reactivity of GGBFS has relationship with phase separation occurring over most of aluminosilicate glasses. The molten slag will separated in to two phases : a silica rich phase with composition close to SiO_2 and an alumina rich phase with composition close to $Al_6Si_2O_{13}$ [22]. With the abundant presence of Ca^{2+}, some researches [23] supposed that Ca rich phase and Si rich phase coexisted in the glass structure of GGBFS, and they found the samples with phase separation have better cementitious reactivity than sample with homogenous glass and sample with crystalline phases. However, there is little testing method to study the phase separation phenomenon directly except electron microscopy techniques, and it is still hard to reach a consensus about the mechanism of separated phases in the hydration process.

It is also well know that the reactions of GGBFS are dominated by small particles. Particles above 20 μm in size react very slowly, while particles below 2 μm react completely within approximately 24 h in blended cements and in alkali-activated systems [24,25].

2.2. Metakaolin (MK)

MK is a pozzolanic material and its use dates back to 1962 when it was incorporated in concrete for Jupia Dam in Brazil. It is a thermally activated aluminosilicate material with high pozzolanic activity comparable to or exceeded the activity of fume silica [26]. And it is generated by calcination of kaolinitic clay at temperature of between 650 °C and 800 °C depending on the purity and crystallinity of the precursor clays [27]. Ambroise et al. [28] demonstrated that MK can also be obtained by the calcination of indigenous lateritic soils at 750–800 °C. Another source for the production of MK is that of calcining waste sludge from the paper recycling industry [29]. The MK sources used in geopolymerization vary markedly in particle size, purity and in the crystallinity of the kaolinite from which they were derived. Generally, the particle size of MK varies to some degree, but is smaller than 5 μm, with the intrinsic size of the clay being in the order of 20 nm. Although the dispersion of particles during mixing will affect the rheological behavior and degree of reaction somewhat, it has been shown that there is little difference in the reaction of alkali-activated MK with variation in raw material surface area [30,31].

Brindley and Nakahira [32,33] studied the phase transformation of kaolinite in the process of calcinations, and MK was obtained at temperature of 500 °C, and transforms to silicon-spinel at 925 °C. When the temperature is above 1400 °C, mullite is generated. It should be noted that silicon-spinel and mullite both have low-activity. The exo-thermal dehydroxylation reactions are represented by Eqs. (2)–(5):

$$\sim 500^\circ C : Al_2O_3 \cdot 2SiO_2 \cdot 2H_2O \rightarrow Al_2O_3 \cdot 2SiO_2 + 2H_2O \qquad (2)$$

$$\text{kaolinite} \qquad\qquad \text{metakaolin}$$

$$925^\circ C : 2[Al_2O_3 \cdot 2SiO_2] \rightarrow 2Al_2O_3 \cdot 3SiO_2 + SiO_2 \qquad (3)$$

$$\text{silicon} - \text{spinel}$$

$$1100^\circ C : 2Al_2O_3 \cdot 3SiO_2 \rightarrow 2[Al_2O_3 \cdot SiO_2] + SiO_2 \qquad (4)$$

$$1 : 1 \text{ mullite} - \text{type phase}$$

$$>1400^\circ C : 3[Al_2O_3 \cdot SiO_2] \rightarrow 3Al_2O_3 \cdot 2SiO_2 + SiO_2 \qquad (5)$$

$$3 : 2 \text{ mullite}$$

MK consists of alternating buckled silicate and aluminate layers, with the silicon in 4-coordination and the aluminum in a mixture of 4-, 5- and 6-coordination. The structure of MK appears disordered to X-ray analysis, although the fact that it is derived by the removal of hydroxyl groups from the layered kaolinite structure means that at some degree of ordering must remain , which is observed by Lee et al.

[34] with Energy-Filtering Transmission Electron Microscopy (EF-TEM) Study. Recently, it is generally accepted that the key to the reactivity of MK is the strain in bonding network induced by thermal dehydroxylation [10], by which changing the coordination number of the aluminum from 6 to a mixture of 4, 5 and 6-coordination [35].

2.3. Comparison of the general properties between GGBFS and MK

GGBFS and MK are both very good pozzolanic materials to produce geopolymers or as additives in OPC. However, the differences in general properties between GGBFS and MK are listed as follows:

(1) "Glass phase" to GGBFS and "amorphous phase" to MK. These are two different concepts. As it is known to all, the glassy of GGBFS is formed by melting and rapid cooling. Fly ash also contains a lot of glass phase by combustion of coal. However, these two kinds of glass phase have different compositions and structure. Generally, the DP of GGBFS glass is lower than fly ash, which means GGBFS has a better activity. While in the case of MK, the crystalline structure is broken down by calcinations at temperatures, which are in general lower than those necessary to generate liquid phase and produce glass on cooling. So "amorphous phase" is appropriate to MK.

(2) Chemical and mineral composition of GGBFS and MK. Generally, the major components of GGBFS are SiO_2, CaO, Al_2O_3 and MgO, which are common components in silicate glasses. While in metakaolin, the two major components are SiO_2 and Al_2O_3. Table 2 summarizes the major chemical composition of GGBFS and metakaolin [36–38]. From the chemical composition, we can consider that GGBFS is $(Si + Ca)$ system and $(Si + Al)$ is suitable for MK. Generally, GGBFS contains massive glass phase, while some crystalline phases may exist in minor level, such as gehlenite, akermanite and merwinite. Nevertheless, MK is ideally synthesized by dehydroxylation of phase pure kaolin, and the base structure is that of highly disrupted phyllosilicate structure containing silicon and aluminum only; although most commercial MK contains levels of impurities, primarily muscovite and titanium dioxide.

3. Hydration products

The hydration products of alkali-activated GGBFS and MK are also very different. It is commonly acknowledged that calcium silicate hydrate (CSH) is the major binding phase in alkali-activated GGBFS. However, the binding property of geopolymers is assumed to be the result of the formation of a three-dimensional zeolite like polymers [39].

The hydration products of alkali-activated GGBFS are controlled by the composition of the slag, the type of activator and PH environment. Wang and Scrivener [40] confirmed that regardless of the activator used, the main hydration product is calcium silicate hydrate (CSH) with low C/S ratio and varying degrees of crystallinity. Puertas et al. [41] studied GGBFS activated with NaOH, and has reported by XRD analysis the presence of hydrotalcite ($Mg_6Al_2CO_3(OH)_{16} \cdot 4H_2O$), calcite ($CaCO_3$) and CSH. Moreover, AFm is also identified in the pastes of slag activated with NaOH [42]. It is interesting to find hydrotalcite is

Table 2
Chemical composition of slag and metakaolin.

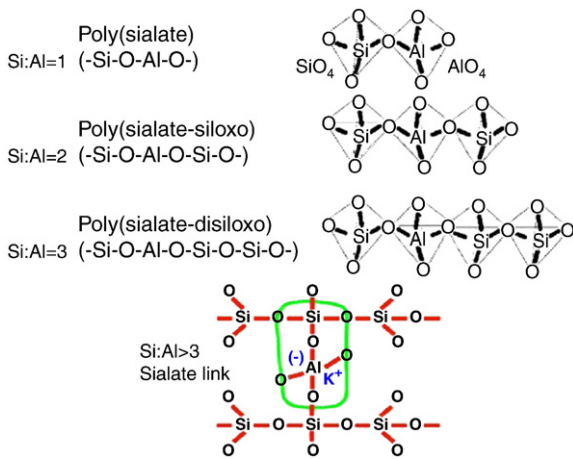| Chemical composition wt.%	GGBFS	Metakaolin
SiO_2,	31–38	49–52
CaO	38–44	–
Al_2O_3	9–13	40–43
MgO	7–12	–

Fig. 1. Poly(sialates) structures according to Davidovits [48].

identified as tiny crystals being closely mixed with CSH gel by many researchers [42–44]. Hydrotalcite starts to form at about 6 h with NaOH and about 12 h with waterglass. While without knowing the exact form in which the Mg and Al exist, it is difficult to discuss the mechanism by which the hydrotalcite is formed [42]. However, Yip et al. [45] found there is no new crystalline peak associated with the alkali activation of GGBFS. Therefore it can be concluded that crystalline CSH is not a product or it is not a dominant product formed as a result of the alkaline activation of GGBFS under the conditions (sodium silicate solution $M_s = 1.2$) used in their investigation. This is in agreement with previous

findings by van Jaarsveld and van Deventer [46] that crystalline CSH is not formed in a high pH (pH > 14) environment.

Mechanism of alkali-activated MK (geopolymers) involves the polycondensation reaction of geopolymeric precursors i.e. alumino-silicate oxide with alkali polysialates yielding polymeric Si–O–Al bond [47,48].

$$M_n\left[-(SiO_2)_z-AlO_2\right]_n, wH_2O$$
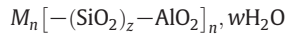
where M is the alkaline element, z is 1, 2, or 3 and n is the degree of polymerization, generating different types of poly(sialates), shown in (Fig. 1).

Many authors [49,50] have found the product of MK activation with NaOH solutions is N–A–S–H gel with good mechanical properties. It has been concluded from FTIR, and ^{27}Al, ^{29}Si MAS-NMR [50] studies that its three-dimensional structure is a network [Q^4(Al)] consisting in alternating SiO_4 and AlO_4 tetrahedra linked by shared O atoms. The general formula for the reaction product is $2SiO_2 \cdot Al_2O_3 \cdot Na_2O \cdot 2H_2O$. When the activator is a NaOH and waterglass mix, the material formed is amorphous and cementitious, but its structure and composition are different from the product formed when NaOH is used alone [51]. In addition, the amorphous N–A–S–H gel has thus similar chemical composition as natural zeolitic materials but without the extensive crystalline zeolitic structure [52–54].

However, what we can confidently state regarding the nanostructure of N–A–S–H gel is: the N–A–S–H gel structure is that of a charge-balance aluminosilicate, which is influenced by the Si/Al ratio and the alkali cations present. In the structure, Al tends to be surrounded by four Si neighbors in a 4-coordinated geopolymer framework. The charge-
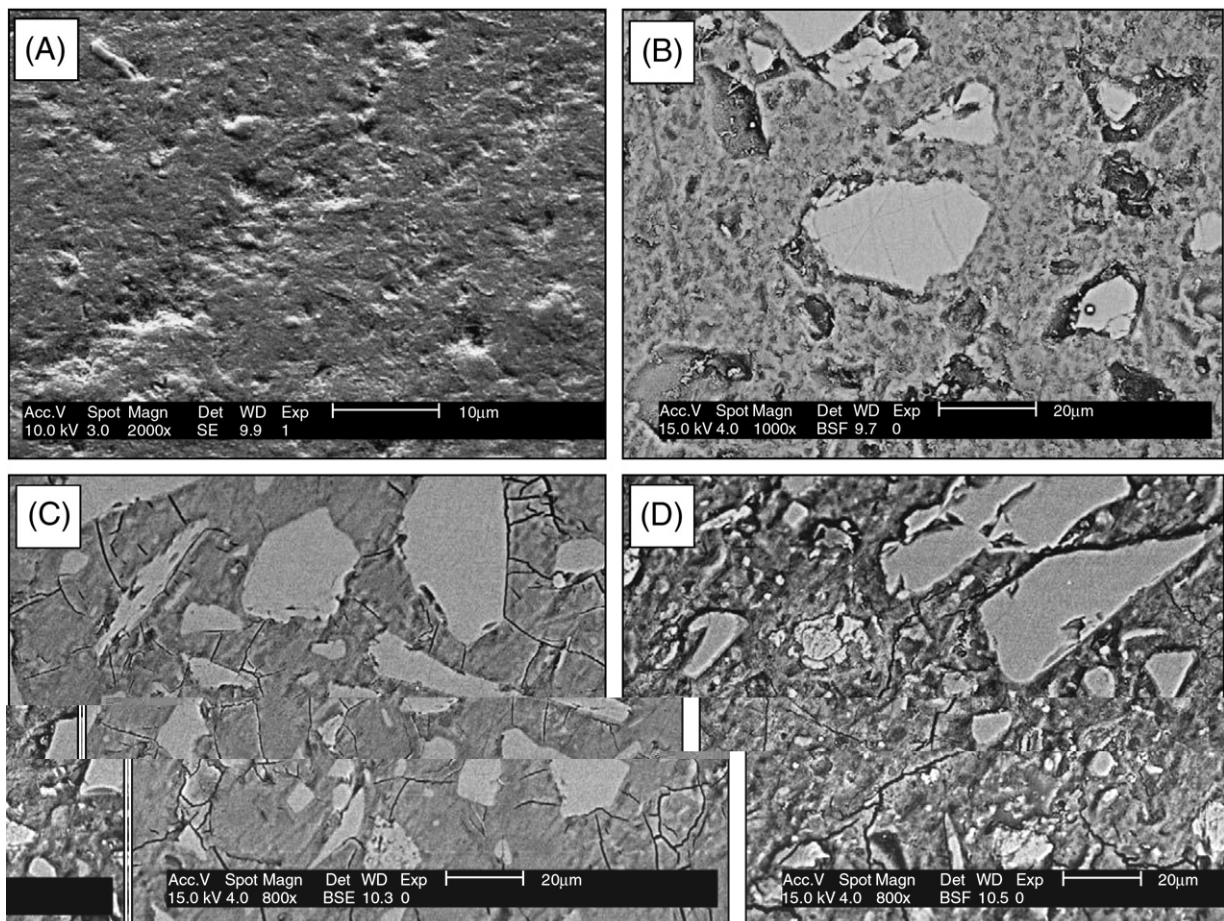

Fig. 2. SEM image of AAK sample (A), AAK–AAS sample (B), AAS sample (C), and PC sample (D) [55].

balanced alkali metal will not associate with the Al atom, but rather will associate with one or more negatively-charged oxygen atoms surrounding the aluminum. As is the case for CSH gel, N–A–S–H gels are difficult to characterize with XRD due to their amorphous or nanocrystalline nature. The use of other techniques such as FTIR, SEM or TEM can furnish valuable information about gel nanostructure and composition [10].

Lecomte [55] compared the microstructure between geopolymers, alkali-activated slag cement and Portland cement, and ^{29}Si MAS-NMR spectroscopy has confirmed that in Portland cement, CSH gel contains silicate groups organised in linear finite chains of "dreierketten" structure, thus mainly SiQ^1 and SiQ^2 species. In alkali-activated slag cement, CSH gel is formed by longer chains in view of the predominance of chain mid-member units, SiQ^2 and $SiQ^2(1Al)$. Geopolymer materials are characterized by a highly polymerized aluminosilicate structure composed mainly of three-dimensional cross-linked units, $SiQ^4(2Al)$ and $SiQ^4(3Al)$.

The micrographs of alkali-activated MK (AAK), slag (AAS), the mixture of them (AAK–AAS) and Portland cement (PC) are shown in Fig. 2(A–D), respectively [55]. Alkali-activated MK sample appears as a homogeneous material while the other samples are composite materials composed of GGBFS particles surrounded by a binding matrix.

4. Reaction mechanisms

4.1. Reaction mechanism of alkali activation of MK

In the 1950's Glukhovsky [56] proposed a general mechanism for the alkali activation of materials primarily comprising silica and reactive alumina. The mechanism of Glukhovsky model is composed of conjoined reactions of destruction–coagulation–condensation–crystallization. The first step consists of a breakdown of the covalent bonds Si–O–Si and Al–O–Si, which happens when the pH of the alkaline solution rises, so those groups are transformed into a colloid phase. Then an accumulation of the destroyed products occurs, which interacts among them to form a coagulated structure, leading in a third phase to the generation of a condensed structure and crystallized. In the recent decades, alkali-activated aluminosilicate materials (geopolymers) have been widely studied. Fig. 3 presents a highly simplified reaction mechanism for geopolymerization. The reaction mechanism shown in Fig. 3 outlines the key processes occurring in the transformation of a solid aluminosilicate source into a synthetic alkali aluminosilicate [30].

The process of alkali activation of MK has been studied by a variety of experimental and modeling techniques over the past two decades. Provis and Deventer [10] summarized the process briefly in their new book:

Alkaline attack on the MK structure results in the release of silicate and aluminate species into solution, with 5- and 6-coordinated Al being converted to 4-coordination upon dissolution [57]. It has been proposed that the initial release of Al may be more rapid than that of Si [58]. The dissolved Al may react with any silicate initially supplied by activating solution, lead to the formation of aluminosilicate oligomers, and this is why use sodium silicate solutions (Na_2O–SiO_2–H_2O) as activating has a better mechanical property than sodium hydroxide (NaOH). Then the N–A–S–H gel grows and eventually begins to crystallize to form zeolites [59].

Fig. 4 [60] presents a simplified model of the reaction processes inspired from Faimon [61] involved in the geopolymerization of MK. The model allows for dissolution of a primary mineral into aluminate and silicate monomers, association of these monomers via both addition and autocatalytic polymerization routes, and formation of an unidentified "secondary mineral" phase. Its extension to geopolymerization is therefore relatively straightforward, requiring only incorporation of the effect of silicate oligomerization (species D) in the concentrated activator solutions, identification of the secondary mineral product G as the amorphous aluminosilicate gel component of the geopolymeric
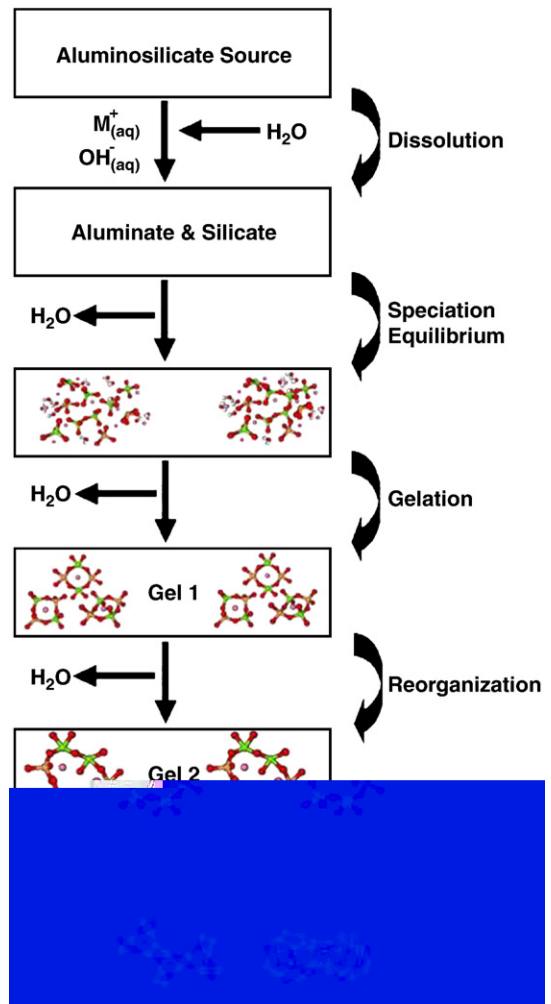

Fig. 3. Conceptual model for alkali activation of aluminosilicate [30].

binder, and inclusion of a second pathway by which the zeolitic phases (Z) observed in geopolymers are formed [60].

4.2. Reaction mechanism of alkali activation of GGBFS

GGBFS contains a reasonable amount of calcium and low aluminum inside the glassy phase, and the reaction mechanism of alkali activation of GGBFS is very different from MK, although it is not widely described as alkali activation of MK.

Alkali hydration of a GGBFS corresponds to a complex process that is composed of several steps, including the initial destruction of the GGBFS and a later polycondensation of the reaction products. Considering the glassy phase contains high Ca and low Al, Fig. 5 provides an illustration of the dissolution mechanism of a glass containing both monovalent and divalent network-modifying cations [16]. The primary distinction between the Na^+ and Ca^{2+} sites shown is the much greater extent of "damage" caused to the glass structure by the removal of a divalent cation than a monovalent one.

Krizan and Zivanovic [61] analyzed the heat release in alkali-activated GGBFS, and have noticed that the higher Na_2O and silica modulus (M_s) were related to higher hydration levels. Meanwhile, the process begins with a destruction of the slag bonds Ca–O, Mg–O, Si–O–Si, Al–O–Al and Al–O–Si, and then a Si–Al layer formed all over the surface of slag grains and, finally, the formation of the hydration products.

The study of Wang et al. [40] indicated that during the hydration of alkali-activated slag, the products form by a dissolution and
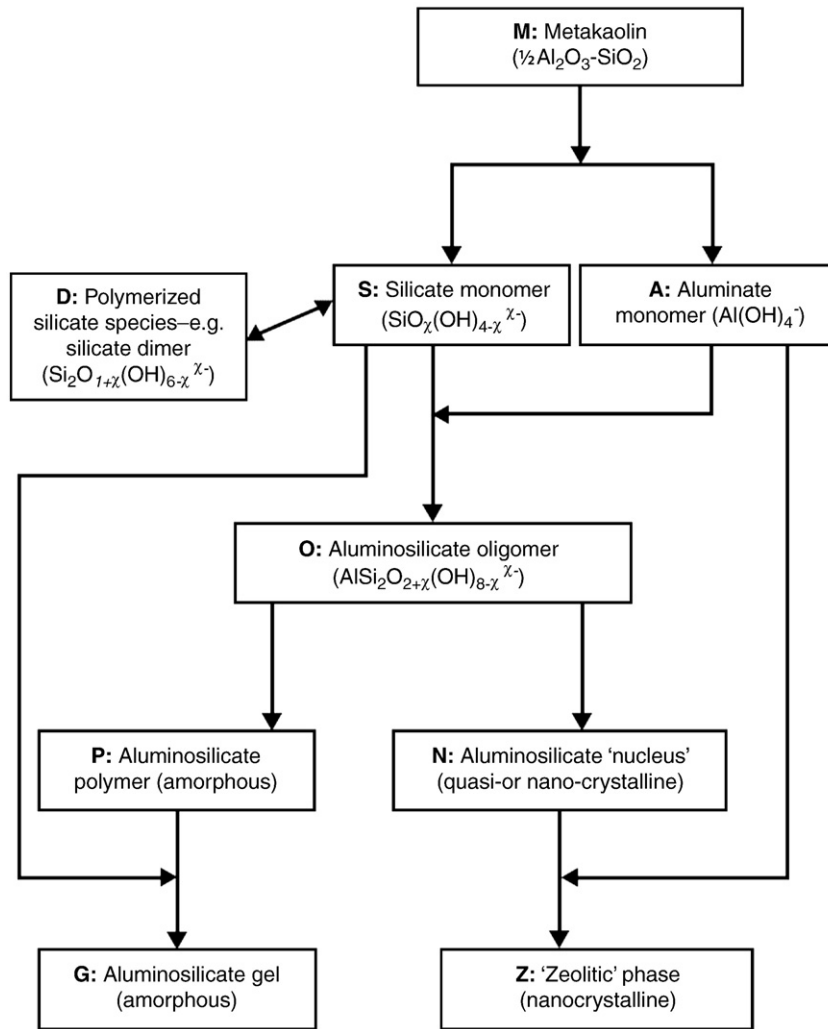
```
┌─────────────────────────────┐
│        M: Metakaolin         │
│       (½Al₂O₃·SiO₂)          │
└─────────────────────────────┘
```

Fig. 4. Schematic outline of the reaction processes involved in geopolymerization [60].

precipitation mechanism during the early stages of reaction, but at later stages the reaction may continue by a solid state mechanism.

Mozgawa and Deja [44] found that during the hydration of alkali-activated slag, the Si^{4+} of sorosilicate units $[Si_2O_7]^{-6}$ in glassy phase are partial substituted by Al^{3+} in tetrahedral positions (typical for melilites), with significant content of amorphous phase by IR spectra. Based on ^{29}Si MAS-NMR spectra, the shift related to Q^2 tetrahedra of pastes indicates the growth of phases composed of tetrahedral chain, mainly CSH. ^{27}Al MAS-NMR spectra prove that as the result of the hydration process, beside the aluminum atoms in tetrahedral co-ordination, the octahedral coordination of these atoms also occurs. The content of aluminum–oxygen octahedral slightly depends on the activator type and the parameters of hydration process.

Obviously, the reaction mechanism of alkali activation of GGBFS is more complicated than geopolymers due to the significant content of calcium. So it is very important to know the role of calcium in GGBFS and hydration process.

4.3. The role of Ca

The effect of calcium on geopolymerization has recently been the subject of a number of detailed investigations [45,50,62]. Recently, ^{43}Ca 3Q and 5QMAS-NMR studies of isotopically enriched synthetic slags have yielded new information on the importance of processing conditions in determining the structure of calcium sites [63]. But it is still unclear how the calcium is structurally bound within the aluminosilicate glass phase. However, the Ca in glassy phase gives an increased tendency toward framework disorder, including the formation of a small concentration (weak, reactive) Al–O–Al bonds if the Al content is sufficiently high, as well as an NBO content higher than is strictly required by stoichiometry [21,64]. And it will decrease the polymerization degree of raw material, seen Eq. (1). This is why GGBFS, rich in Ca^{2+} as modifiers, provides an excellent raw material for alkali activation than Class C or Class F fly ash.

Various studies [45,65] have found that calcium has a positive effect on the comprehensive strength of geopolymeric binds, and the role of Ca on geopolymerization has recently been the subject of investigation. The amount of Ca in the raw materials and the form in which it is present both play significant roles in determining the reaction pathway and the physical properties of the final hydration products. It has been reported that the formation of Ca compounds in geopolymers is greatly dependent on the pH and Si/Al ratio [45,62].

Song et al. [66,67] studied the pore solution of alkali-activated GGBFS by NaOH combined with thermodynamic calculation, and they found the solubility of Si increased with pH while that of Ca decreased. Thus, in the very beginning of alkali activation of GGBFS, the active silicate ions react with Ca^{2+} forming CSH with a low Ca/Si ratio. Table 3 shows atomic ratios from EDS X-ray microanalysis in the SEM for C–S–H gels formed in different conditions [43]. It was found that the Ca/Si ratio of CSH at 1–7 days and 1 year were the same and a little
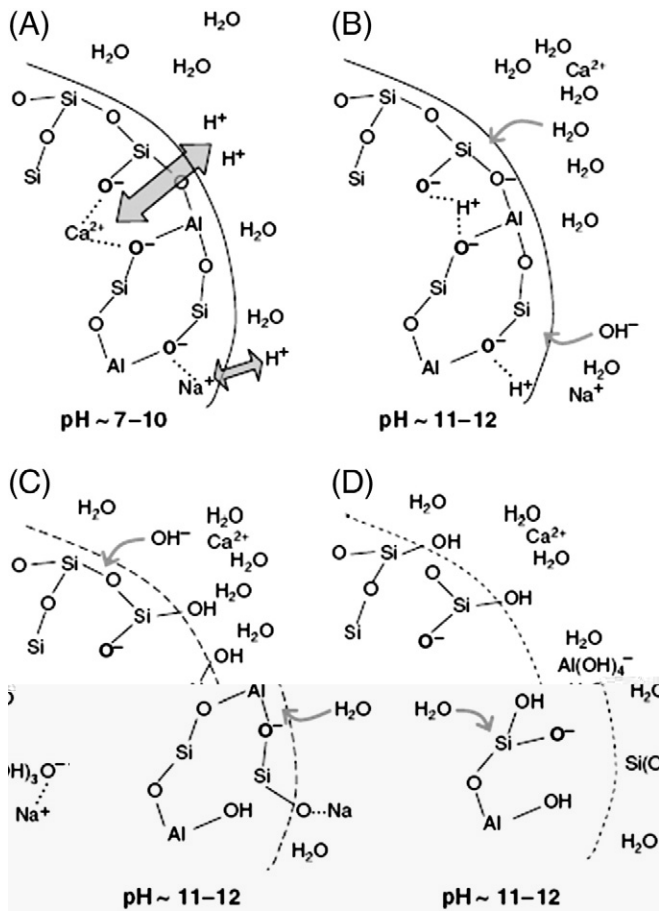
Fig. 5. Dissolution mechanism of an aluminosilicate glass during the early stage of reaction: (A) exchange of H⁺ for Ca²⁺ and Na⁺, (B) hydrolysis of Al–O–Si bonds, (C) breakdown of the depolymerized glass network, and (D) release of Si and Al. Charged framework oxygen sites are marked in bold; note the charge transfer reaction occurring between panels (B) and (C), and proton transfer throughout. All framework Si and Al sites are tetrahedrally coordinated to oxygen, but additional bonds are not shown for clarity [16].
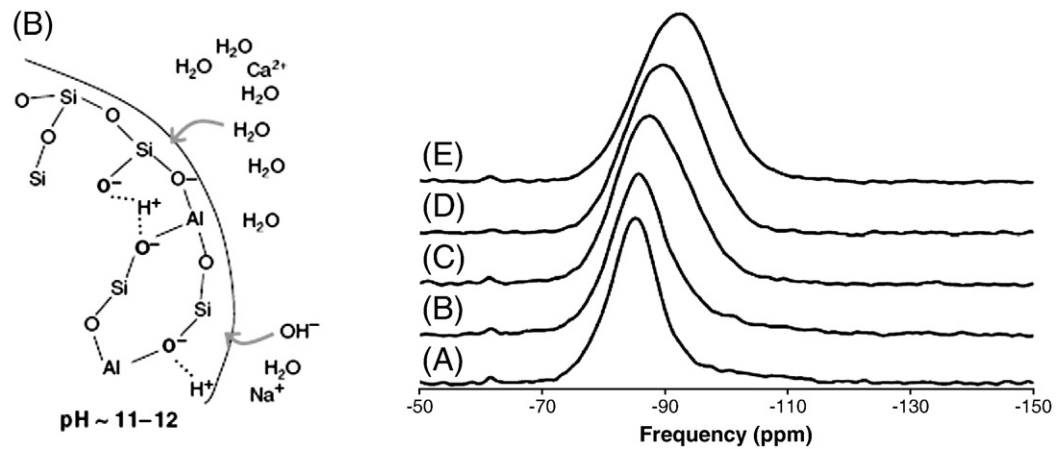

Fig. 6. ^{29}Si MAS-NMR spectra of Na-geopolymer with Si/Al of (A) 1.15, (B) 1.40, (C) 1.65, (D) 1.90, and (E) 2.15 [72].

lower than that of raw GGBFS with Ca/Si 1.21, which suggested that the CSH formed with a constant Ca/Si ratio at the beginning of hydration and the rest of Ca may reacted with Al to form AFm.

The calcium hydroxide–metakaolin system is in itself of interest as a means of analyzing the pozzolanic reaction in Portland cement concrete. The addition of a sufficient quantity of Ca to geopolymers in the form of calcium hydroxide can lead to the formation of phase-separated Al-substitute calcium silicate hydrate (C–(A)–S–H) and geopolymer (N–A–S–H) gels [45,50,62]. This is known to be more prevalent at relatively low alkalinity conditions system, because if the OH⁻ concentration is high, the dissolution of Ca(OH)₂ is hindered and it is also possible that very highly alkaline conditions will lead to dissolution of any C–S–H type phases which are formed. It has also been suggested that Ca²⁺ is capable of acting as charge-balancing cation within the geopolymeric binding structure, but it needs to be further studied.

4.4. The role of Al

In the alkali-activated cements, Al plays an important role. It is well known that the availability of aluminum controls to a large degree the properties of geopolymers [68,69]. The absolute amount of available aluminum and the rate of its release throughout reaction not only affect final strength, but other properties in the wet and hardened states including setting characteristics, flexural strength, acid resistance, microstructure, and strength development profile.

Generally, there are about 10% aluminum oxide in slag and 40% in metakaolin. According to the differences in the hydration products and, obviously, the role of Al in these two systems is different.

Thermodynamic calculations and sorption/speciation arguments [70] show that most Al(IV)–O–Si bonds are more readily broken than Si–O–Si bonds. The glassy phase of GGBFS most likely to provide aluminum during hydration are these depolymerized glasses. In the alkali-activated GGBFS with NaOH pastes, aluminum is present in CSH gel as 4-coordination and combined with magnesium in hydrotalcite or AFm as 6-coordination [43]. ^{27}Al MAS-NMR spectra of initial slag samples show amorphous phase, mainly with 4-coordination of aluminum. The hydration process with activators leads to the occurrence of aluminum atoms in 6-coordination. It seems that a relative increase in the tetrahedral configuration content, with prolongation of hydration time, is a simple consequence of an increase in the amount of aluminum incorporated into the C–S–H phase, caused by disintegration of slag glass, being influenced by the presence of sodium ions. Additionally, hydrothermal conditions do not favor crystallization of aluminate-ions-containing phases, on the contrary they facilitate decomposition of an aluminosilicate structure, with the creation of C–S–H phase, containing substitutions of silicon with aluminum, which supports the creation of tobermorite phase. While a relative increase in aluminum in 6-coordination proves an increase in hydrotalcite amount, instead of aluminum-containing CSH [44]. Wang discussed the role of Al in the system of alkali activation of GGBFS. In the initial stage of hydration, aluminum tends to go preferentially into hydrotalcite, and depending on the Ca/Si ratio of the system, the extra Al may form AFm and /or go into CSH structure [42].

However, MK is known to contain approximately equal populations of Al(IV), Al(V) (~30 ppm) and Al(VI). It is observed that during the course of alkali-mediated reaction, Al(V) and Al(VI) are converted to tetrahedral sites with an associated alkali cation to maintain electroneutrality [71]. Duxson et al. [72] reported that increasing in Si/Al ratio caused the $SiQ^4(mAl)$ positions to shift to higher frequencies, shown in Fig. 6. So it can be concluded Al may substituted for Si of about 3, presented as $SiQ^4(3Al)$ type three-dimensional cross-linked structure, which was also confirmed by other authors [73,74]. This

Table 3
Atomic ratios from EDS X-ray microanalysis in the SEM for CSH gels formed in different conditions (raw GGBFS: Ca/Si 1.21, Al/Si 0.41) [43].

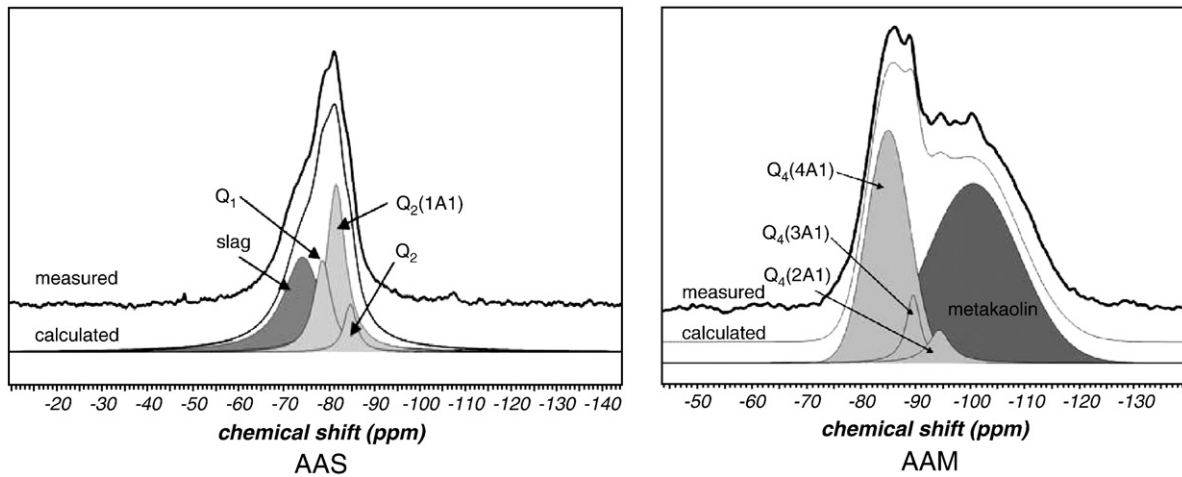| Alkalis	Waterglass		NaOH	
Age	1–7 days	1 year	1–7 days	1 year
Ca/Si of CSH	1.0	1.0	1.1	1.1
Al/Si of CSH	0.20	0.21	0.18	0.20

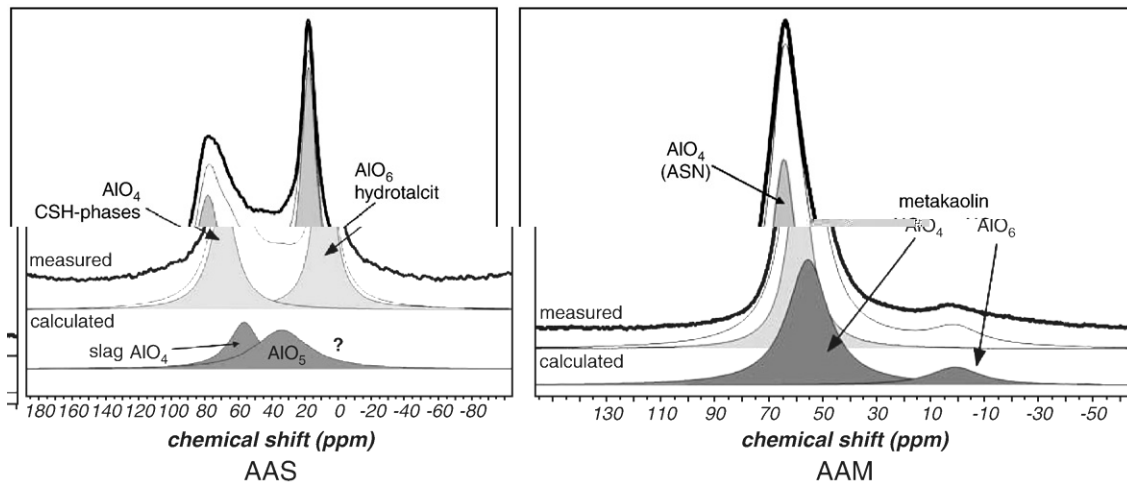Fig. 7. ^{29}Si NMR spectrum and interpretation of the alkali-activated GGBFS (AAS) and MK (AAM) [36].

Fig. 8. ^{27}Al NMR spectrum and interpretation of the alkali-activated GGBFS (AAS) and MK (AAM) [36].

is different to alkali-activated GGBFS, in which CSH gel is formed in view of the predominance of chain mid-member units, $SiQ^2(1Al)$ and $SiQ^2(0Al)$.

In addition, Buchwald et al. [36] compared ^{29}Si, ^{27}Al NMR spectrum of alkali-activated GGBFS and MK, shown in Figs. 7 and 8. The alkaline activated MK (AAM) reacted to form an amorphous structure showing, only Q^4-Signals in the ^{29}Si NMR spectrum and 4-coordinated aluminum in the ^{27}Al NMR spectrum. The main appearance of signals from structures is $SiQ^4(4Al)$. The alkaline activated GGBFS reacted to form C–S–H phases (with incorporated aluminum), revealed as Q^1 and Q^2 in the ^{29}Si NMR spectrum and 4-coordinated aluminum in the ^{27}Al NMR spectrum, as well as to hydrotalcite which was seen as six-coordinated aluminum in the ^{27}Al NMR spectrum and confirmed by X-ray diffraction.

5. Conclusions

Based on varies researches on alkali-activated cements, it is generally accepted that they are two different concepts of alkali-activated GGBFS and geopolymer. Alkali activation of GGBFS is a model of (Si + Ca) system, and geopolymer is a kind of (Si + Al) cement with metakaolin and fly ash as main material. The present paper compares the differences between these two cements, mainly on their general properties, hydration products and reaction mechanism.

Both of these two materials have been widely studied. However, for GGBFS, much remains to be discovered regarding the specific network structure of the phases present in each type of slag, and especially the role of Ca in glassy structure and the hydration process. While for metakaolin, the main drawback is that the very high surface area and plate-like particle shape of the metakaolin mean that the water demand is very high, which in turn causes difficulties related to drying shrinkage and cracking.

In a word, much work of geopolymer has been done, yet much work remains to be done. It is hoped that future research progress in this field will drive the commercial utilization of geopolymer in the construction industry.

References

[1] D.M. Roy, Alkali-activated cements: opportunities and challenges, Cem. Concr. Res. 29 (1999) 249–254.
[2] P. Krivenko, Alkaline cements: terminology classification, aspects of durability, in: H. Justnes (Ed.), Proceedings of the 10th International Congress on the Chemistry of Cement, Gothenburg, Sweden, Amarkai and Congrex Göteborg, Gothenburg, Sweden, 1997, p. 6, 4iv046.
[3] J. Deja, Immobilization of Cr^{6+}, Cd^{2+}, Zn^{2+} and Pb^{2+} in alkali-activated slag binders, Cem. Concr. Res. 32 (2002) 1971–1977.
[4] J.W. Cho, K. Ioku, S. Goto, Effect of PbII and CrVI on the hydration of slag-alkaline cement and the immobilization of these heavy metal ions, Adv. Cem. Res. 11 (1999) 111–116.
[5] G. Qian, D.D. Sun, J.H. Tay, Characterization of mercury- and zinc-doped alkali-activated slag matrix, part I. Mercury, Cem. Concr. Res. 33 (8) (2003) 1251–1256.

[6] G. Qian, D.D. Sunand, J.H. Tay, Characterization of mercury- and zinc-doped alkali-activated slag matrix, part II, Zinc, Cem. Concr. Res. 33 (8) (2003) 1257–1262.

[7] A. Palomo, M.W. Grutzek, M.T. Blanco, Alkali-activated fly ashes: a cement for the future, Cem. Concr. Res. 29 (1999) 1323–1329.

[8] J. Davidovits, Properties of Geopolymer Cements, in: P.V. Krivenko (Ed.), Proceedings of First International Conference on Alkaline Cements and Concretes, Kiev, Ukraine, 1, 1994, pp. 131–149.

[9] C. Shi, P.V. Krivenko, D.M. Roy, Alkali-Activated Cements and Concrete, Taylor & Francis, London and New York, 2006.

[10] J. Provis, J. Van Deventer, Geopolymers: Structure, Processing, Properties and Industrial Applications, Woodhead Publishing Limited, UK, 2009.

[11] I.D. Balon, Y.F. Nikulin, V.N. Muravev, V.M. Antipov, N.M. Mishchen, Slag formation in production of steelmaking pig-iron, Steel in the USSR 4 (1973) 268–273.

[12] N.Y. Mostafa, S.A.S. El-Hemaly, E.I. Al-Wakeel, S.A. El-Korashy, P.W. Brown, Characterization and evaluation of the hydraulic activity of water-cooled slag and air-cooled slag, Cem. Concr. Res. 31 (2001) 899–904.

[13] D. Li, Z. Xu, Z. Luo, Z. Pan, C. Lin, The activation and hydration of glassy cementitious materials, Cem. Concr. Res. 32 (2002) 1145–1152.

[14] R.N. Swamy, A. Bouikni, Some engineering properties of slag concrete as influenced by mix proportioning and curing, ACI Mater. J. 87 (1990) 210–220.

[15] S.C. Pal, A. Mukherjee, S.R. Pathak, Investigation of hydraulic activity of ground granulated blast furnace slag in concrete, Cem. Concr. Res 33 (2003) 1481–1486.

[16] P. Duxson, J.L. Provis, Designing precursors for geopolymer cements, J. Am. Ceram. Soc. 91 (12) (2008) 3864–3869.

[17] B.O. Mysen, Structure and Properties of Silicate Melts, Elsevier, Amsterdam, 1988.

[18] S.K. Lee, G.D. Cody, B.O. Mysen, Structure and the extent of disorder in quaternary (Ca–Mg and Ca–Na) aluminosilicate glasses and melts, Am. Mineral. 90 (2005) 1393–1401.

[19] B.O. Mysen, P. Richet, Silicate Glasses and Melts: Properties and Structure (Developments in Geochemistry), Elsevier, Amsterdam, 2005.

[20] J. Allwardt, S.K. Lee, J.F. Stebbins, Bonding preferences of nonbridging oxygens in calcium aluminosilicate glass: evidence from O-17MAS and 3QMAS NMR on calcium aluminate glass, Am. Mineral. 88 (2003) 949–954.

[21] S.K. Lee, J.F. Stebbins, Disorder and the extent of polymerization in calcium silicate and aluminosilicate glasses: O-17 NMR results and quantum chemical molecular orbital calculations, Geochim. Cosmochim. Ac. 70 (2006) 4275–4286.

[22] S. Aramaki, R. Roy, Revised phase diagram for the system Al_2O_3–SiO_2, J. Am. Ceram. Soc. 45 (1961) 229–242.

[23] Y. Li, H.H. Sun, X.M. Liu, Z.D. Cui, Effect of phase separation structure on cementitious reactivity of blast furnace slag, Sci. China, Ser. E 52 (2009) 2695–2699.

[24] H. Wan, Z. Shui, Z. Lin, Analysis of geometric characteristics of GGBS particles and their influences on cement properties, Cem. Concr. Res. 34 (2004) 133–137.

[25] P.Z. Wang, R. Trettin, V. Rudert, Effect of fineness and particle size distribution of granulated blast-furnace slag on the hydraulic reactivity in cement systems, Adv. Cem. Res. 17 (2005) 161–166.

[26] A.A. Caldaron, R.G. Burg, High-reactivity metakaolin: a new generation mineral, Concr. Int. 11 (1994) 37–40.

[27] J. Pera, Metakaolin and calcined clays, Cem. Concr. Compos 23 (2001) iii.

[28] J. Ambroise, M. Murat, J. Pera, Hydration reaction and hardening of calcined clays and related minerals: V. Extension of the research and general conclusions, Cem. Concr. Res. 15 (1985) 261–268.

[29] R. García, R. Vigil de la Villa, I. Vegas, M. Frías, M.I. Sánchez de Rojas, The pozzolanic properties of paper sludge waste, Constr. Build. Mater. 22 (2008) 1484–1490.

[30] P. Duxson, A. Fernández-Jiménez, J.L. Provis, G.C. Lukey, A. Palomo, J.S.J. van Deventer, Geopolymer technology: the current state of the art, J. Mater. Sci. 42 (2007) 2917–2933.

[31] H. Rahier, J.F. Denayer, B. van Mele, Low-temperature synthesized aluminosilicate glasses — Part IV — modulated DSC study on the effect of particle size of metakaolinite on the production of inorganic polymer glasses, J. Mater. Sci. 38 (2003) 3131–3136.

[32] G.W. Brindley, M. Nakahira, A new concept of the transformation sequence of kaolinite to mullite, Nature 181 (1958) 1333–1334.

[33] G.W. Brindley, M. Nakahira, The kaolinite–mullite reaction series: IV, The coordination of Aluminum, J. Am. Ceram. Soc. 44 (1961) 506–507.

[34] S. Lee, Y.J. Kim, H.S. Moon, Energy-filtering transmission electron microscopy (EF-TEM) study of a modulated structure in metakaolinite, represented by a 14 Å modulation, J. Am. Ceram. Soc. 86 (2003) 174–176.

[35] K.J.D. MacKenzie, D.R.M. Brew, R.A. Fletcher, R. Vagana, Formation of aluminosilicate geopolymers from 1:1 layer-lattice minerals pre-treated by various methods: a comparative study, J. Mater. Sci. 42 (2007) 4667–4674.

[36] A. Buchwald, H. Hilbig, Ch. Kaps, Alkali-activated metakaolin–slag blends — performance and structure in dependence of their composition, J. Mater. Sci. 42 (2007) 3024–3032.

[37] Zongjin Li, Zhu Ding, Property improvement of Portland cement by incorporating with metakaolin and slag, Cem. Concr. Res. 33 (2003) 579–584.

[38] T.W. Cheng, J.P. Chiu, Fire-resistant geopolymer produced by granulated blast furnace slag, Miner. Eng. 16 (2003) 205–210.

[39] F. Pacheco-Torgal, J. Castro-Gomes, S. Jalali, Alkali-activated binders: a review. Part 1. Historical background, terminology, reaction mechanisms and hydration products, Constr. Build. Mater. 22 (2008) 1305–1314.

[40] S.-D. Wang, K.L. Scrivener, Hydration products of alkali activated slag cement, Cem. Concr. Res. 25 (1995) 561–571.

[41] F. Puertas, A. Fernández-Jiménez, M.T. Blanco-Varela, Pore solution in alkali-activated slag cement pastes. Relation to the composition and structure of calcium silicate hydrate, Cem. Concr. Res. 34 (2004) 195–206.

[42] S-D. Wang, Alkaline activation of slag, PhD Thesis, Imperial College, University of London, 1995.

[43] S.-D. Wang, K.L. Scrivener, ^{29}Si and ^{27}Al NMR study of alkali-activated slag, Cem. Concr. Res. 33 (2003) 769–774.

[44] W. Mozgawa, J. Deja, Spectroscopic studies of alkaline activated slag geopolymers, J. Mol. Struct. 924–926 (2009) 434–441.

[45] C.K. Yip, G.C. Lukey, J.S.J. van Deventer, The coexistence of geopolymeric gel and calcium silicate hydrate at the early stage of alkaline activation, Cem. Concr. Res. 35 (2005) 1688–1697.

[46] J.G.S. van Jaarsveld, J.S.J. van Deventer, Effect of the alkali metal activator on the properties of fly ash-based geopolymers, Ind. Eng.Chem. Res. 38 (1999) 3932–3941.

[47] J.G.S. Van Jaarsveld, J.S.J. Van Deventer, L. Lorenzen, The potential use of geopolymeric materials to immobilise toxic metals: Part I. Theory and applications, Miner. Eng. 10 (1997) 659–669.

[48] J. Davidovits, Geopolymer chemistry and sustainable development, the poly (sialate) terminology: a very useful and simple model for the promotion and understanding of green-chemistry, Proceedings of 2005 Geopolymere Conference, 1, 2005, pp. 9–15.

[49] M.L. Granizo, M.T. Blanco, F. Puertas, A. Palomo, Alkaline activation of metacaolin: influence of synthesis parameters, Proceeding of the Tenth International Congress on Chemistry of Cement, Göteborg, vol. 3, 1997, p. 3ii113.

[50] M.L. Granizo, S. Alonso, M.T. Blanco-Varela, A. Palomo, Alkaline activation of metakaolin: effect of calcium hydroxide in the products of reaction, J. Am. Ceram. Soc. 85 (1) (2002) 225–231.

[51] H. Rahier, W. Simons, B. van Mele, M. Biesemans, Recent literature in geopolymer science and technology, J. Mater. Sci. 32 (9) (1997) 2237–2247.

[52] J. Davidovits, Chemistry of geopolymeric systems, terminology, Geopolymer'99 Second International Conference Saint-Quentin, France, 1999, pp. 9–39.

[53] I. Lecomte, M. Liegeois, A. Rulmont, R. Cloots, F. Maseri, Synthesis and characterization of newinorganic polymeric composites based on kaolin or white clay and on ground-granulated blast furnace slag, J. Mater. Res. 18 (2003) 2571–2579.

[54] V.F.F. Barbosa, K.J.D. Mackensie, C. Thaumaturgo, Synthesis and characterisation of materials based on inorganic polymers of alumina and silica: sodium polysialate polymers, Int. J. Inorg. Mater. 2 (2000) 309–317.

[55] I. Lecomte, C. Henrist, M. Liégeois, F. Maseri, A. Rulmont, R. Cloots, (Micro)-structural comparison between geopolymers, alkali-activated slag cement and Portland cement, J. Eur. Ceram. Soc. 26 (2006) 3789–3797.

[56] V.D. Glukhovsky, G.S. Rostovskaja, G.V. Rumyna, High strength slag alkaline cements, Proceedings of the Seventh International Congress on the Chemistry of Cement, 3, 1980, pp. 164–168.

[57] P. Duxson, G.C. Lukey, F. Separovic, J.S.J. van Deventer, Effect of alkali cations on aluminum incorporation in geopolymeric gels, Ind. Eng. Chem. Res. 44 (4) (2005) 832–839.

[58] L. Weng, K. Sagoe-Crentsil, Dissolution processes, hydrolysis and condensation reactions during geopolymer synthesis: Part I — low Si/Al ratio systems, J. Mater. Sci. 42 (2007) 2997–3006.

[59] P. Duxson, S.W. Mallicoat, G.C. Lukey, W.M. Kriven, J.S.J. van Deventer, The effect of alkali and Si/Al ratio on the development of mechanical properties of metakaolin-based geopolymers, Colloids Surf., A 292 (2007) 8–20.

[60] J.L. Provis, P. Duxon, J.S.J. Van Deventer, G.C. Lukey, The role of mathematical modeling and gel chemistry in advancing geopolymer technology, Chem. Eng. Res. Des. 83 (2005) 853–860.

[61] J. Faimon, Oscillatory silicon and aluminum aqueous concentrations during experimental aluminosilicate weathering, Geochim. Cosmochim. Acta 60 (1996) 2901–2907.

[62] C.K. Yip, G.C. Lukey, J.L. Provis, J.S.J. van Deventer, Effect of calcium silicate sources on geopolymerisation, Cem. Concr. Res. 38 (2008) 554–564.

[63] K. Shimoda, Y. Tobu, K. Kanehashi, T. Nemoto, K. Saito, Total understanding of the local structures of an amorphous slag: perspective from multi-nuclear (^{29}Si, ^{27}Al, ^{17}O, ^{25}Mg, and ^{43}Ca) solid-state NMR, J. Non-Cryst. Solids 354 (2008) 1036–1043.

[64] J.F. Stebbins, Z. Xu, NMR evidence for excess non-bridging oxygen in an aluminosilicate glass, Nature 390 (6655) (1997) 60–62.

[65] H. Xu, J.S.J. Van Deventer, The geopolymerisation of alumino-silicate minerals, Int. J. Miner. Process. 59 (2000) 247–266.

[66] S. Song, H.M. Jennings, Pore solution chemistry of alkali-activated ground granulated blast-furnace slag, Cem. Concr. Res. 29 (1999) 159–170.

[67] S. Song, D. Sohn, H.M. Jennings, T.O. Mason, Hydration of alkali-activated ground granulated blast furnace slag, J. Mater. Sci. 35 (2000) 249–257.

[68] P. Duxson, A. Fernández-Jiménez, J.L. Provis, G.C. Lukey, A. Palomo, J.S.J. Deventer, Geopolymer technology: the current state of the art, J.Mater. Sci. 42 (9) (2007) 2917–2933.

[69] A. Fernández-Jiménez, A. Palomo, I. Sobrados, J. Sanz, The role played by the reactive alumina content in the alkaline activation of fly ashes, Micropor. Mesopor. Mater. 91 (1–3) (2006) 111–119.

[70] J.P. Hamilton, S.L. Brantley, C.G. Pantano, L.J. Criscenti, J.D. Kubicki, Dissolution of nepheline, jadeite and albite glasses: toward better models for aluminosilicate dissolution, Geochim. Cosmochim. Acta 65 (21) (2001) 3683–3702.

[71] J. Davidovits, Geopolymers: inorganic polymeric new materials, J. Therm. Anal. 37 (8) (1991) 1633–1656.

[72] P. Duxson, J.L. Provis, G.C. Lukey, F. Separovic, J.S.J. van Deventer, ^{29}Si NMR study of structural ordering in aluminosilicate geopolymer gels, Langmuir 21 (2005) 3028–3036.

[73] H. Rahier, W. Simons, B. van Mele, M. Biesemans, Low-temperature synthesized aluminosilicate glasses.3. Influence of the composition of the silicate solution on production, structure and properties, J. Mater. Sci. 32 (9) (1997) 2237–2247.

[74] M. Luz Test, Alkali activation of metakaolins: parameters affecting mechanical, structural and microstructural properties, J. Mater. Sci. 42 (9) (2007) 2934–2943.